Meccanica (2013) 48:275–285
DOI 10.1007/s11012-012-9599-1

Radiation effects on mixed convection about a cone embedded in a porous medium filled with a nanofluid

Ali J. Chamkha · S. Abbasbandy · A.M. Rashad · K. Vajravelu

Received: 2 November 2011 / Accepted: 25 August 2012 / Published online: 19 September 2012

Abstract The problem of steady, laminar, mixed convection boundary-layer flow over a vertical cone embedded in a porous medium saturated with a nanofluid is studied, in the presence of thermal radiation. The model used for the nanofluid incorporates the effects of Brownian motion and thermophoresis with Rosseland diffusion approximation. The cone surface is maintained at a constant temperature and a constant nanoparticle volume fraction. The resulting governing equations are non-dimensionalized and transformed into a non-similar form and then solved by Keller box method. A comparison is made with the available results in the literature, and our results are in very good agreement with the known results. A parametric study of the physical parameters is made and a representative set of numerical results for the local Nusselt and Sherwood numbers are presented graphically. Also, the salient features of the results are analyzed and discussed.

Keywords Mixed convection · Nanofluid · Thermophoresis · Brownian diffusion · Thermal radiation

A.J. Chamkha
Manufacturing Engineering Department, The Public Authority for Applied Education and Training, Shuweikh 70654, Kuwait

S. Abbasbandy (✉)
Department of Mathematics, Imam Khomeini International University, Ghazvin, Iran
e-mail: abbasbandy@yahoo.com

A.M. Rashad
Department of Mathematics, Faculty of Science, South Valley University, Aswan, Egypt

K. Vajravelu
Department of Mathematics, University of Central Florida, Orlando, FL 32816, USA

1 Introduction

Fluid flow and heat transfer in porous media received considerable interest during the last several decades. This is primarily because of the numerous applications of flow through porous medium, such as storage of radioactive nuclear waste, transpiration cooling, separation processes in chemical industries, filtration, transport processes in aquifers, groundwater pollution, geothermal extraction, fiber insulation, etc. Theories and experiments of thermal convection in porous media and state-of-the-art reviews, with special emphasis on practical applications are presented in the recent books by Nield and Bejan [1], Vafai [2], Pop and Ingham [3], Ingham and Pop [4] and Bejan et al. [5]. Yih [6, 7] examined coupled heat and mass transfer by free convection over a truncated cone in porous media. Cheng [8] studied natural convection heat and mass transfer from a vertical truncated cone in a porous medium saturated with a non-Newtonian fluid with variable wall temperature and concentration. Cheng [9] also analyzed Soret and Dufour effects on

natural convection boundary layer flow over a vertical cone in a porous medium with constant wall heat and mass fluxes.

On the other hand, nanofluids are prepared by dispersing solid nanoparticles in base fluids such as water, oil, or ethylene glycol. These fluids are used in an innovative way to increase thermal conductivity and, thereby, heat transfer. Unlike heat transfer in conventional fluids, the exceptionally high thermal conductivity of nanofluids provides for exceptional heat transfer, a unique feature of nanofluids. Advances in device miniaturization have necessitated heat transfer systems that are small in size, light mass, and high performance. Several authors have tried to establish convective transport models for nanofluids. The comprehensive references on nanofluid can be found in the recent book by Das et al. [10] and in the review papers by Buongiorno [11], Bianco et al. [12], and Nield and Kuznetsov [13–17]. Xuan et al. [18] have examined the transport properties of nanofluid and have expressed that thermal dispersion, which takes place due to the random movement of particles, takes a major role in increasing the heat transfer rate between the fluid and the wall. This requires a thermal dispersion coefficient, which is still unknown. Brownian motion of the particles, ballistic phonon transport through the particles and nanoparticle clustering can also be the possible reason for this enhancement is presented by Keblinski and Phillpot [19]. Das et al. [20] has observed that the thermal conductivity for a nanofluid increases with increasing temperature. They have also observed the stability of Al_2O_3–water and CuO–water nanofluids. Experiments on heat transfer due to natural convection with nanofluid have been studied by Putra et al. [21] and Wen and Ding [22]. They have observed that heat transfer decreases with increase in concentration of nanoparticles. The viscosity of this nanofluid increases rapidly with the inclusion of nanoparticles as the shear rate decreases. Chamkha et al. [23] have studied mixed convection MHD flow of a nanofluid past a stretching permeable surface in the presence of magnetic field, heat generation or absorption, thermophoresis, Brownian motion and suction or injection effects. Chamkha et al. [24] have also analyzed natural convection past a sphere embedded in a porous medium saturated by a nanofluid. Gorla et al. [25] have studied the boundary layer flow of a nanofluid on a stretching circular cylinder in a stagnant free stream. Also, Gorla et al. [26] have analyzed mixed convection past a vertical wedge embedded in a porous medium saturated by a nanofluid. Chamkha et al. [27] investigated the problem of steady mixed convection flow of a nanofluid adjacent to an isothermal wedge embedded in a saturated porous medium in the presence of thermal radiation with Rosseland diffusion approximation. If confirmed and found consistent, they would use nanofluids for application in thermal management. Furthermore, suspensions of metal nanoparticles are also being developed for other purposes, such as medical applications including cancer therapy. The interdisciplinary nature of nanofluid research presents a great opportunity for exploration and discovery at the frontiers of nanotechnology. Also, the nanofluids are widely used as coolants, lubricants, heat exchangers and micro-channel heat sinks. Nanofluids usually contain the nanoparticles such as metals, oxides or carbon nanotubes; whereby these nanoparticles have unique chemical and physical properties.

However, the thermal radiation effect on mixed convection heat transfer in porous media is very important in high-temperature processes and has many important applications such as space technology, geothermal engineering, the sensible heat storage bed, the nuclear reactor cooling system, and underground nuclear wastes disposal. Yih [28, 29] studied radiation effect on mixed convection over an isothermal wedge/cone in porous media. Bakier [30] presented an analysis of the thermal radiation effect on stationary mixed convection from vertical surfaces in saturated porous media. Kumari and Nath [31] studied the radiation effect on the non-Darcy mixed convection flow over a non-isothermal horizontal surface in a porous medium. Chamkha and Ben-Nakhi [32] studied the mixed convection–radiation interaction along a permeable surface immersed in a porous medium. The problem of hydromagnetic heat transfer by mixed convection from melting of a vertical plate in a liquid saturated porous medium, taking into account the effects of thermal radiation, was investigated by Bakier et al. [33].

Motivated by these studies, in this paper, the effect of thermal radiation on mixed convection boundary-layer flow over an isothermal vertical cone embedded in a porous medium saturated with a nanofluid is considered. The model used for the nanofluid incorporates the effects of Brownian motion and thermophoresis with Rosseland diffusion approximation. Numerical solutions of the boundary layer equations are obtained and discussion is provided for several values of

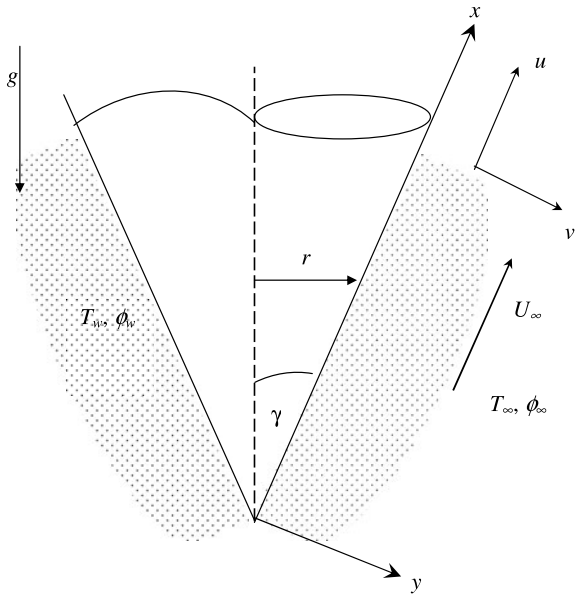

Fig. 1 Flow model and physical coordinate system

the nanofluid parameters governing the problem. The dependency of local Nusselt number and local Sherwood number on these parameters are discussed.

2 Problem formulation

Consider the problem of the radiation effect on mixed-convection boundary-layer flow of optically dense viscous incompressible nanofluid over an isothermal vertical cone (with half angle γ) embedded in a saturated porous medium. The model used for the nanofluid incorporates the effects of Brownian motion and thermophoresis. The uniform wall temperature of the cone T_w and uniform nanoparticle volume fraction ϕ_w are higher than the ambient temperature T_∞ and ambient nanoparticle volume fraction ϕ_∞, respectively. The flow over the cone is assumed to be two-dimensional, laminar, steady, and incompressible. Figure 1 shows the flow model and the physical coordinate system. The porous medium is assumed to be uniform, isotropic and in local thermal equilibrium with the fluid. All fluid properties are assumed to be constant. In the laminar sub-layer near the wall, Brownian diffusion and thermophoresis are important for nanoparticles of any material and size, see Buongiorno [11]. For nanofluids, in Cartesian coordinates system of x and y the governing steady conservation of follows under the Boussinesq and the, thermal energy with Rosseland diffusion approximations and nanoparticles equations including the dynamic effects of nanoparticles can be written as (see Yih [34, 35] and Nield and Kuznetsov [14]):

$$\frac{\partial(ru)}{\partial x}+\frac{\partial(rv)}{\partial y}=0, \tag{1}$$

$$\frac{\partial u}{\partial y}=\frac{(1-\phi_\infty)\rho_{f\infty}\cos\gamma\beta g K}{\mu}\frac{\partial T}{\partial y} - \frac{(\rho_p-\rho_{f\infty})\cos\gamma g K}{\mu}\frac{\partial\phi}{\partial y}, \tag{2}$$

$$u\frac{\partial T}{\partial x}+v\frac{\partial T}{\partial y} =\alpha\frac{\partial^2 T}{\partial y^2}+\tau\left[D_B\frac{\partial\phi}{\partial y}\frac{\partial T}{\partial y}+\left(\frac{D_T}{T_\infty}\right)\left(\frac{\partial T}{\partial y}\right)^2\right] + \frac{16\sigma}{3(a_r+\sigma_s)(c_p\rho)_f}\frac{\partial}{\partial y}\left(T^3\frac{\partial T}{\partial y}\right), \tag{3}$$

$$u\frac{\partial\phi}{\partial x}+v\frac{\partial\phi}{\partial y}=D_B\frac{\partial^2\phi}{\partial y^2}+\left(\frac{D_T}{T_\infty}\right)\frac{\partial^2 T}{\partial y^2}, \tag{4}$$

where x and y denote the vertical and horizontal directions, respectively. u, v, T and ϕ are the x and y components of velocity, temperature and nanoparticle volume fraction, respectively. K, β, D_B and D_T are the permeability of the porous medium, volumetric expansion coefficient of fluid, the Brownian diffusion coefficient and thermophoretic diffusion coefficient, respectively. μ, ρ_f and ρ_p are the fluid viscosity, fluid density and the nanoparticle mass density, respectively. g, σ, σ_s, and a_r are the acceleration due to gravity, the Stefan–Boltzmann constant, scattering coefficient, and the Rosseland mean extinction coefficient, respectively. $\alpha=k/(\rho c)_f$ and $\tau=(\rho c)_p/(\rho c)_f$ are the thermal diffusivity of porous medium and the ratio of heat capacities, respectively. k, $(\rho c)_f$ and $(\rho c)_p$ are thermal conductivity, heat capacity of the fluid and the effective heat capacity of nanoparticle material, respectively. The last term on the right side of the energy equation (3) is the thermal radiation heat flux and is approximated using the Roseland diffusion equation. Details of the derivation of Eqs. (3) and (4) are given in the articles by Buongiorno [11] and Nield and Kuznetsov [13–17].

The appropriate boundary conditions suggested by the physics of the problem are

$$y=0: \quad v(x,0)=0, \quad T=T_w, \quad \phi=\phi_w, \tag{5a}$$

$$y\to\infty: \quad u=U_\infty, \quad T=T_\infty, \quad \phi=\phi_\infty, \tag{5b}$$

where T_w and ϕ_w are the wall temperature and wall nanoparticle volume fraction, respectively. T_∞ and ϕ_∞ are the free stream velocity, temperature and nanoparticle volume fraction, respectively. We assume that the boundary layer thickness is sufficiently thin in comparison with the local radius of the cone. Hence, the local radius to a point in the boundary layer can be replaced by the radius of the cone r, i.e., $r = x\sin\gamma$. For cone flow, $U_\infty = Bx^m$ is the velocity of the potential flow outside the boundary layer. Here, B is a prescribed constant and $m = (\gamma/\pi - \gamma)$ is the cone angle parameter. The tabulated values γ and m are given by Hess and Faulkner [36]. The cone angles of 15 °, 45° and 75° are discussed in this paper, therefore, $m = 0.0316314, 0.2450773, 0.6667277$. It is convenient to transform the governing equations into a non-similar dimensionless form which can be studied as an initial-value problem. This can be done by introducing the stream function: $u = \partial\psi/\partial y$, $v = -\partial\psi/\partial x$ and using

$$\begin{aligned}
&\eta = \frac{y}{x}\left(\mathrm{Pe}_x^{1/2}\right)\chi^{-1},\\
&\chi = \left(1+\left(\frac{\mathrm{Ra}_x}{\mathrm{Pe}_x}\right)^{1/2}\right)^{-1} \psi = \alpha\left(\mathrm{Pe}_x^{1/2}\right)\chi^{-1}S(\chi,\eta),\\
&\theta = \frac{T-T_\infty}{T_w-T_\infty},\\
&f = \frac{\phi-\phi_\infty}{\phi_w-\phi_\infty}, \qquad \mathrm{Pe}_x = U_\infty x/\alpha,\\
&\mathrm{Ra}_x = \left\{(1-\phi_\infty)\rho_{f\infty} g\beta_T K(T_w-T_\infty)x/\mu\alpha\right\},
\end{aligned} \tag{6}$$

where Pe_x and Ra_x are the local Peclet and modified Rayleigh numbers, respectively. χ is the mixed convection parameter, ψ is the stream function, S is the dimensionless stream function, f is the dimensionless nanoparticle volume fraction, and θ is the dimensionless temperature. Using the expressions in (6), we can write Eqs. (1)–(5a), (5b) as

$$S'' = (1-\chi)^2\left(\theta' - \mathrm{N_r} f'\right), \tag{7}$$

$$\begin{aligned}
&\theta'' + \frac{1}{2}(3+m\chi)S\theta' + \mathrm{N_b} f'\theta' + \mathrm{N_t}\theta'^2\\
&\quad + \frac{4\mathrm{R_d}}{3}\left\{\theta'\left[(H-1)\theta+1\right]^3\right\}'\\
&\quad = \frac{m}{2}\chi(1-\chi)\left(S'\frac{\partial\theta}{\partial\chi} - \theta'\frac{\partial S}{\partial\chi}\right),
\end{aligned} \tag{8}$$

$$\begin{aligned}
&f'' + \frac{\mathrm{Le}}{2}(3+m\chi)Sf' + \frac{\mathrm{N_t}}{\mathrm{N_b}}\theta''\\
&\quad = \frac{\mathrm{Le}}{2}m\chi(1-\chi)\left(S'\frac{\partial f}{\partial\chi} - f'\frac{\partial S}{\partial\chi}\right),
\end{aligned} \tag{9}$$

$$(3+m\chi)S(\chi,0) + m\chi(1-\chi)\frac{\partial S(\chi,0)}{\partial\chi} = 0, \tag{10a}$$

$$\begin{aligned}
&\theta(\chi,0) = 1, \qquad f(\chi,0) = 1,\\
&S'(\chi,\infty) = \chi^2, \qquad \theta(\chi,\infty) = 0,\\
&f(\chi,\infty) = 0,
\end{aligned} \tag{10b}$$

where

$$\begin{aligned}
&\mathrm{Le} = \frac{\alpha}{D_B}, \qquad \mathrm{N_r} = \frac{(\rho_p-\rho_{f\infty})(\phi_w-\phi_\infty)}{(1-\phi_\infty)\rho_{f\infty}\beta(T_w-T_\infty)},\\
&\mathrm{N_b} = \frac{\varepsilon(\rho c)_p D_B(\phi_w-\phi_\infty)}{(\rho c)_f\alpha},\\
&\mathrm{N_t} = \frac{\varepsilon(\rho c)_p D_T(T_w-T_\infty)}{(\rho c)_f\alpha T_\infty},\\
&\mathrm{R_d} = 4\sigma T_\infty^3/\left[k(a_r+\sigma_s)\right], \qquad H = T_w/T_\infty,
\end{aligned} \tag{11}$$

are the Lewis number, buoyancy ratio, Brownian motion parameter, thermophoresis parameter, conduction-radiation parameter and the surface temperature excess ratio, respectively. It should be noted that $\chi = 0$ ($\mathrm{Pe}_x = 0$) corresponds to pure free convection while $\chi = 1$ ($\mathrm{Ra}_x = 0$) corresponds to pure forced convection. The entire regime of mixed convection corresponds to values of χ between 0 and 1. Most nanofluids examined to date have large values for the Lewis number $\mathrm{Le} > 1$ (see Nield and Kuznetsov [14]). For water nanofluids at room temperature with nanoparticles of 1–100 nm diameters, the Brownian diffusion coefficient D_B ranges from 4×10^{-4} to 4×10^{-12} $\mathrm{m}^{-2}/\mathrm{s}$. Furthermore, the ratio of Brownian diffusivity coefficient to thermophoresis coefficient for particles with diameters of 1–100 nm can be varied in the ranges of 2–0.02 for alumina, and from 2 to 20 for copper nanoparticles (see Buongiorno [11] for details). Hence, the variation of non-dimensional parameters of nanofluids in the present study is considered to vary in the mentioned range.

Of special significance for this problem are the local Nusselt and Sherwood numbers. These physical quantities can be defined as:

$$\begin{aligned}
\mathrm{Nu}_x &= \frac{hx}{k} = \frac{q_w x}{(T_w-T_\infty)}\\
&= -\theta'(\chi,0)\left(\mathrm{Ra}_x^{1/2}+\mathrm{Pe}_x^{1/2}\right)\left(1+\frac{4\mathrm{R_d}H^3}{3}\right)
\end{aligned} \tag{12}$$

$$\text{or} \quad \frac{\mathrm{Nu}_x}{\mathrm{Ra}_x^{1/2}+\mathrm{Pe}_x^{1/2}} = -\theta'(\chi,0)\left(1+\frac{4\mathrm{R_d}H^3}{3}\right),$$

Table 1 Comparison of values of $-(1+(4\mathrm{R_d}H^3/3))\theta'(\chi,0)$ for various values of m and χ in the absence of nanoparticles volume fraction, Brownian motion and thermophoresis effects ($\mathrm{N_r}=\mathrm{N_b}=\mathrm{N_t}=0$) for $\mathrm{R_d}=0.5$ and $H=1.1$

χ	Yih [28]			Present results		
	$m=0.0316314$	$m=0.2450773$	$m=0.6667277$	$m=0.0316314$	$m=0.2450773$	$m=0.6667277$
0.0	1.0380	1.0380	1.0380	1.0380	1.0380	1.0380
0.1	0.9438	0.9444	0.9452	0.9438	0.9444	0.9452
0.2	0.8728	0.8751	0.8788	0.8728	0.8751	0.8788
0.3	0.8301	0.8357	0.8449	0.8301	0.8357	0.8449
0.4	0.8196	0.8301	0.8480	0.8196	0.8301	0.8480
0.5	0.8423	0.8589	0.8883	0.8423	0.8589	0.8883
0.6	0.8960	0.9191	0.9614	0.8960	0.9192	0.9615
0.7	0.9758	1.0054	1.0604	0.9758	1.0054	1.0605
0.8	1.0761	1.1117	1.1783	1.0761	1.1117	1.1784
0.9	1.1919	1.2328	1.3097	1.1920	1.2329	1.3097
1.0	1.3192	1.3648	1.4508	1.3193	1.3649	1.4509

Table 2 Comparison of values of $-(1+(4\mathrm{R_d}H^3/3))\theta'(\chi,0)$ for various values of m and χ in the absence of nanoparticles volume fraction, Brownian motion and thermophoresis effects ($\mathrm{N_r}=\mathrm{N_b}=\mathrm{N_t}=0$) for $\mathrm{R_d}=5$ and $m=0.1156458$

χ	Yih [28]			Present results		
	$H=1.1$	$H=2$	$H=3$	$H=1.1$	$H=2$	$H=3$
0.0	2.3359	4.6459	7.9247	2.3359	4.6461	7.9256
0.1	2.1243	4.2194	7.1931	2.1243	4.2196	7.1944
0.2	1.9651	3.8845	6.6096	1.9651	3.8847	6.6107
0.3	1.8705	3.6658	6.1192	1.8706	3.6660	6.2160
0.4	1.8493	3.5834	6.0547	1.8500	3.5823	6.0523
0.5	1.9038	3.6463	6.1209	1.9038	3.6463	6.1196
0.6	2.0282	3.8475	6.4246	2.0283	3.8476	6.4293
0.7	2.2113	4.1676	6.9427	2.2114	4.1677	6.9435
0.8	2.4404	4.5822	7.6197	2.4405	4.5823	7.6209
0.9	2.7040	5.0684	8.4213	2.7041	5.0685	8.4226
1.0	2.9929	5.6076	9.3114	2.9931	5.6080	9.3172

$$\begin{aligned}\mathrm{Sh}_x &= \frac{h_m x}{D_\mathrm{B}} = \frac{m_\mathrm{w} x}{(\phi_\mathrm{w}-\phi_\infty)} \\ &= -f'(\chi,0)\left(\mathrm{Ra}_x^{1/2}+\mathrm{Pe}_x^{1/2}\right) \\ \text{or}\quad \frac{\mathrm{Sh}_x}{\mathrm{Ra}_x^{1/2}+\mathrm{Pe}_x^{1/2}} &= -f'(\chi,0).\end{aligned} \tag{13}$$

where q_w and m_w are the heat transfer and mass transfer, respectively at the cone surface are given by:

$$\begin{aligned}q_\mathrm{w} &= \left[\left(k+\frac{16\sigma T^3}{3(a_\mathrm{r}+\sigma_\mathrm{s})(c_\mathrm{p}\rho)_\mathrm{f}}\right)\frac{\partial T}{\partial y}\right]_{y=0}, \\ m_\mathrm{w} &= D_\mathrm{B}\left(\frac{\partial \phi}{\partial y}\right)_{y=0}.\end{aligned} \tag{14}$$

3 Numerical method and validation

The governing equations (7), (8) and (9) with the boundary conditions (10a), (10b) are non-linear partial differential equations. The system of Eqs. (7)–(9) are

Table 3 Comparison of values of $-(1+(4\mathrm{R_d}H^3/3))\theta'(\chi,0)$ for various values of m and χ in the absence of nanoparticles volume fraction, Brownian motion and thermophoresis effects ($\mathrm{N_r}=\mathrm{N_b}=\mathrm{N_t}=0$) for $H=3$ and $m=0.4241237$

χ	Yih [28]			Present results		
	$\mathrm{R_d}=0$	$\mathrm{R_d}=5$	$\mathrm{R_d}=10$	$\mathrm{R_d}=0$	$\mathrm{R_d}=5$	$\mathrm{R_d}=10$
0.0	0.7686	7.9248	11.1798	0.7686	7.9256	11.1814
0.1	0.6997	7.1980	10.1538	0.6997	7.1989	10.1562
0.2	0.6496	6.6302	9.3510	0.6497	6.6315	9.3554
0.3	0.6228	6.2657	8.8340	0.6229	6.2676	8.8411
0.4	0.6222	6.1413	8.6624	0.6222	6.1446	8.6666
0.5	0.6480	6.2739	8.8444	0.6480	6.2782	8.8538
0.6	0.6975	6.6486	9.3755	0.6975	6.6532	9.3814
0.7	0.7661	7.2317	10.1966	0.7661	7.2329	10.1984
0.8	0.8491	7.9692	11.2361	0.8480	7.9705	11.2231
0.9	0.9427	8.8239	12.4412	0.9427	8.8257	12.4434
1.0	1.0440	9.7658	13.7655	1.0440	9.7674	13.7709

solved numerically using an implicit finite difference scheme known as the Keller box method as described by Cebeci and Bradshaw [37]. The computations were carried out with $\Delta\chi=0.01$ and $\Delta\eta=0.01$ (uniform grids). The value of $\eta_\infty=50$ is found to be sufficiently enough to obtain the accuracy of $|\theta'(0)|<10^{-5}$.

In order to validate the numerical results, comparisons with the previously published results of Yih [28] for the case of Newtonian fluid are made when $\mathrm{R_d}=\mathrm{N_r}=\mathrm{N_b}=\mathrm{N_t}=0$. These comparisons are presented in Tables 1, 2 and 3. From these tables we see the excellent agreement between our results and the available results in the literature. Table 4 shows the numerical results obtained by variable grid with initial step size $\Delta\eta_1=0.01$ and variable grid parameter of 1.01.

Table 4 Comparison of values of $-(1+(4\mathrm{R_d}H^3/3))\theta'(\chi,0)$ for various values of m and χ in the absence of nanoparticles volume fraction, Brownian motion and thermophoresis effects ($\mathrm{N_r}=\mathrm{N_b}=\mathrm{N_t}=0$) for $\mathrm{R_d}=0.5$, $H=1.1$ and $m=0.0316314$

χ	Yih [28]	Present results (uniform grid)	Present results (variable grid)
0.0	1.0380	1.0380	1.0380
0.1	0.9438	0.9438	0.9439
0.2	0.8728	0.8728	0.8729
0.3	0.8301	0.8301	0.8302
0.4	0.8196	0.8196	0.8194
0.5	0.8423	0.8423	0.8422
0.6	0.8960	0.8960	0.8958
0.7	0.9758	0.9758	0.9757
0.8	1.0761	1.0761	1.0760
0.9	1.1919	1.1920	1.1918
1.0	1.3192	1.3193	1.3192

4 Results and discussion

In this section, representative numerical results are displayed with the help of graphical illustrations. Computations were carried out for various values of physical parameters such as the buoyancy ratio $\mathrm{N_r}$, the Brownian motion parameter $\mathrm{N_b}$, the thermophoresis parameter $\mathrm{N_t}$, the free stream velocity exponent m, the surface temperature parameter H, the radiation–conduction parameter $\mathrm{R_d}$, the Lewis number Le, and the mixed convection parameter χ.

Figures 2a and 2b show the effects of the buoyancy ratio parameter $\mathrm{N_r}$ on the local Nusselt number and the local Sherwood number, for the entire range of the mixed convection parameter $0\le\chi\le1$ for various values of $\mathrm{N_r}$. It is seen that an increase in the buoyancy ratio enhances both the local Nusselt and the Sherwood numbers. Moreover, the parameter $\mathrm{N_r}$ appears only in the momentum boundary layer equation (7). Buoyancy is principally a macroscale effect. The buoyancy influences the velocity and the temperature fields, however, has a minor effect on nanoparticle diffusion. This explains the minor influence of buoyancy on volume fraction nanoparticle profiles. How-

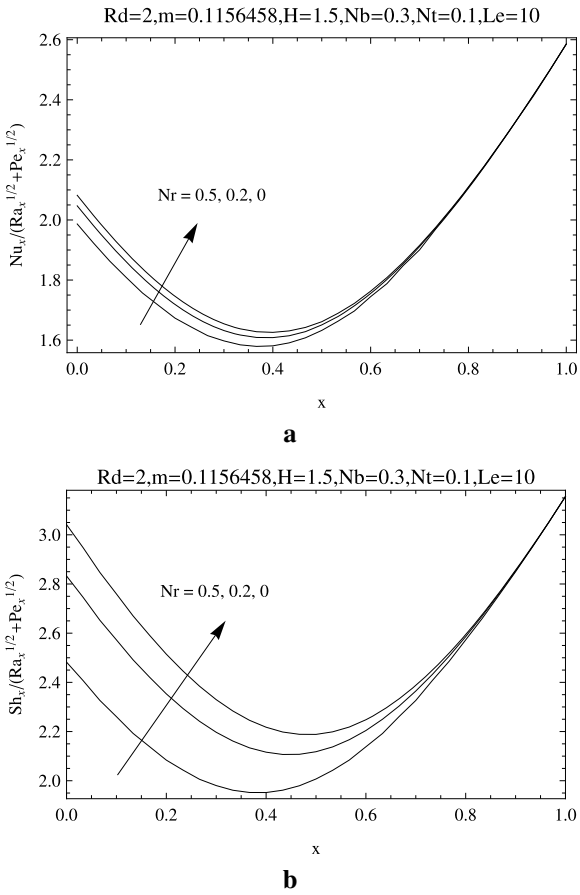

Fig. 2 Effect of N_r on **a** the local Nusselt number and **b** the local Sherwood number

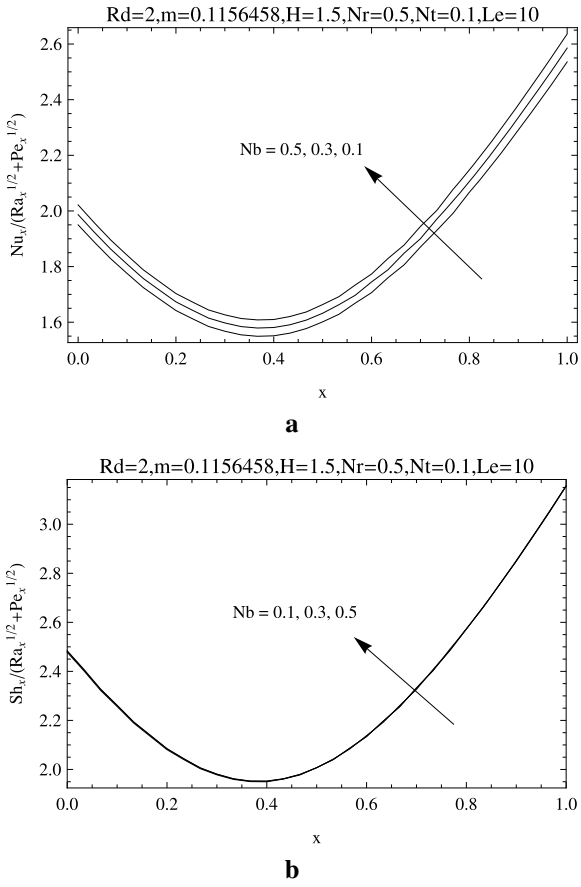

Fig. 3 Effect of N_b on **a** the local Nusselt number and **b** the local Sherwood number

ever, for $\chi = 1$ (forced convection limit), the flow is uncoupled from the thermal and volume fraction buoyancy effects and therefore, there is no change in the local Nusselt and Sherwood numbers for all values of N_r. From the definition of χ, it is observed that an increase in the value of the parameter Ra_x/Pe_x causes the mixed convection parameter χ to decrease. Thus, small values of Ra_x/Pe_x correspond to values of χ close to unity which indicate almost pure forced convection regime. On the other hand, high values of Ra_x/Pe_x correspond to values of χ close to zero, indicate almost pure free convection regime. Furthermore, moderate values of Ra_x/Pe_x represent values of χ between 0 and 1 which correspond to the mixed convection regime. For the forced convection limit ($\chi = 1$), it is clear from Eq. (7) that the velocity in the boundary layer is uniform. However, for smaller values of χ (higher values of Ra_x/Pe_x) at a fixed value of N_r, the buoyancy effect increases.

Figures 3a and 3b illustrate the changes in the local Nusselt number $-(1 + (4R_d H^3/3))\theta'(\chi, 0)$ and local Sherwood number $-f'(\chi, 0)$ for various values of the Brownian motion parameter N_b for the entire range of the mixed convection parameter $0 \leq \chi \leq 1$, respectively. It can be seen that as the Brownian motion parameter N_b increases both the local Nusselt number and local Sherwood number. In nanofluid systems, owing to the size of the nanoparticles, Brownian motion takes place, and this can enhance the heat transfer properties. This is due to the fact that the Brownian diffusion promotes heat conduction. The nanoparticles increase the surface area for heat transfer. Nanofluid is a two phase fluid where the nanoparticles move randomly and increase the energy exchange rates. However, the Brownian motion reduces nanoparticle diffusion. The increase in the local Sherwood number as

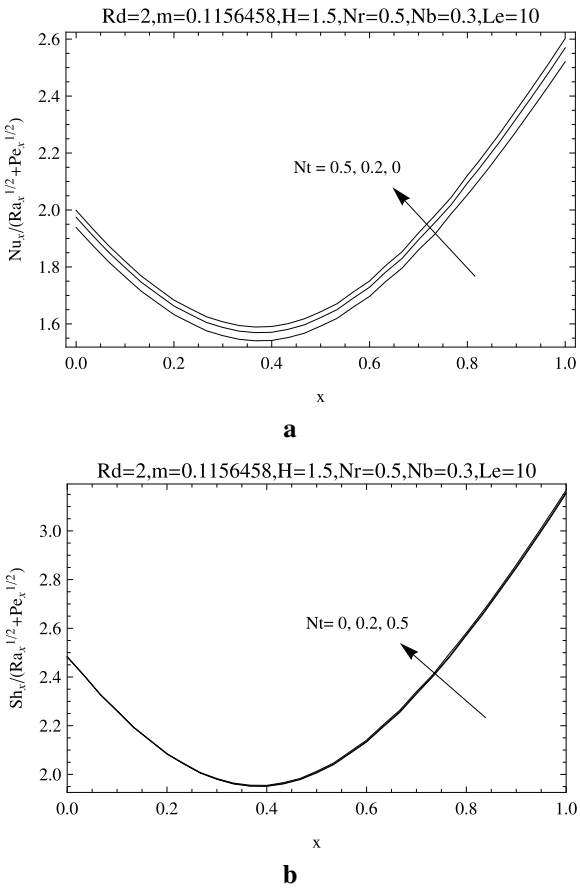

Fig. 4 Effect of N_t on **a** the local Nusselt number and **b** the local Sherwood number

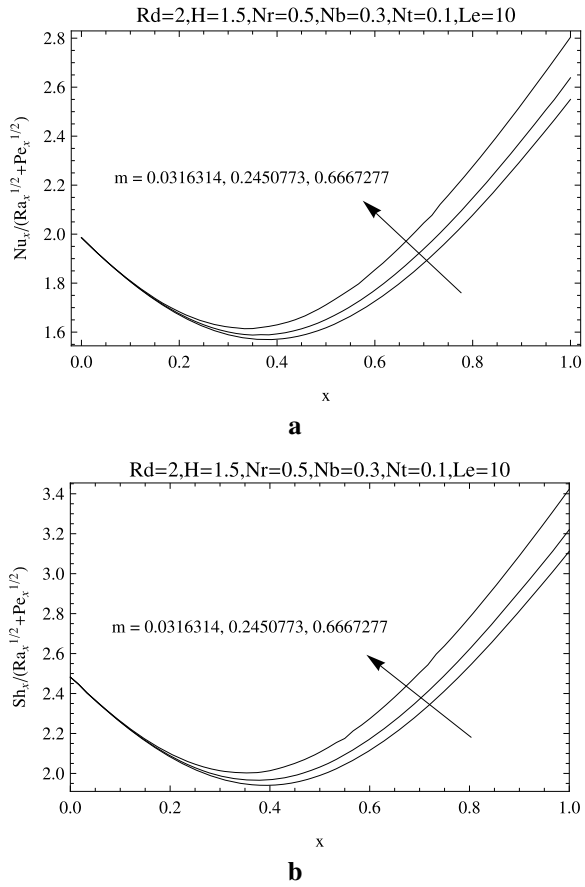

Fig. 5 Effect of m on **a** the local Nusselt number and **b** the local Sherwood number

N_b changes is relatively small. This is due to the large value of Le. In addition, when the mixed convection parameter χ is changed from 0 to 1, the local Nusselt and Sherwood numbers initially decrease reaching corresponding minimum values in the range $0 \leq \chi \leq 1$ and then increase gradually. This phenomenon of a minimum in the local Nusselt number (or Sherwood number) has been explained in the work of Hsieh et al. [38] for the problem of mixed convection flow over a vertical flat plate.

Figures 4a and 4b depict the influence of the thermophoresis parameter N_t on N_u and Sh, respectively. It can be seen that the thermophoresis parameter, N_t appears in the thermal and concentration boundary layer equations. As we note, it is coupled with the temperature function and plays a strong role in determining the diffusion of heat and nanoparticle concentration in the boundary layer. An increase in the values of the thermophoresis parameter N_t results in increasing the values of $-(1+(4R_d H^3/3))\theta'(\chi,0)$ and $-f'(\chi,0)$.

Figures 5a and 5b show representatively the effects of the free stream velocity exponent (cone angle parameter) m on the local Nusselt number $-(1+(4R_d H^3/3))\theta'(\chi,0)$ and on the local Sherwood number $-f'(\chi,0)$ in the entire range for the mixed convection parameter $(0 \leq \chi \leq 1)$. From these figures we see that an increase in the free stream velocity exponent m causes enhancements in both the heat and mass transfer, and as result in the local Nusselt and the Sherwood numbers: This is true for the entire range $0 < \chi < 1$. However, it is noticed that the effect of m on the local Nusselt and the Sherwood numbers are almost negligible for the free convection limit $(\chi = 0)$. This phenomenon is consistent with and also reported by Kumari and Gorla [39] in their work on combined

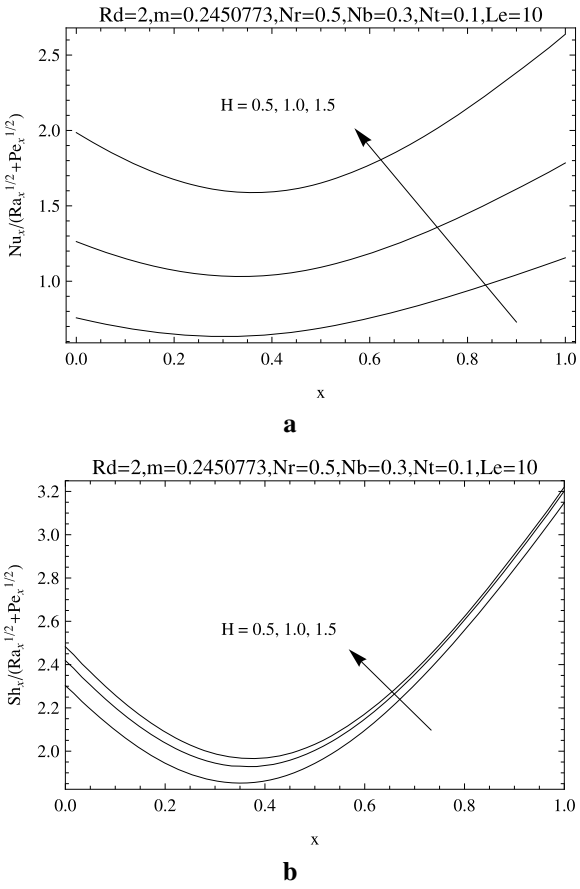

Fig. 6 Effect of H on **a** the local Nusselt number and **b** the local Sherwood number

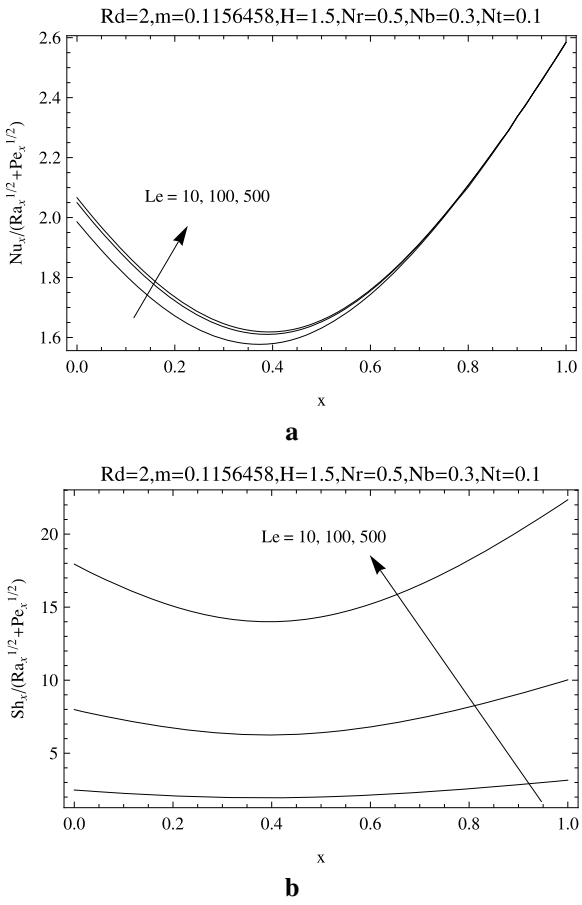

Fig. 7 Effect of Le on **a** the local Nusselt number and **b** the local Sherwood number

convection along a non-isothermal wedge in a porous medium.

Figures 6a and 6b present the effect the surface temperature parameter H on the values of the local Nusselt and the Sherwood numbers in the entire range of the mixed convection parameter $0 \leq \chi \leq 1$, respectively. It can be observed from these figures that the values of both the local Nusselt and the Sherwood numbers increase as the value of H increases: This is true in the entire range $0 < \chi < 1$. However, the effect of H is almost negligible on the local Sherwood number; but more pronounced with the local Nusselt number.

Figures 7a and 7b display the effects of the Lewis number Le on the local Nusselt number and on the local Sherwood number for the entire range of the mixed convection parameter $0 \leq \chi \leq 1$, respectively. It is observed that, an increase in the Lewis number Le causes a reduction in the local Nusselt number and an enhancement in the local Sherwood number.

Figures 8a and 8b show the effect of the radiation-conduction parameter $\mathrm{R_d}$ on the local Nusselt number for both cases of Newtonian and nanofluids in the entire range of the mixed convection parameter $0 \leq \chi \leq 1$, respectively. It is found that the local Nusselt number and the Sherwood number increase with increasing value of $\mathrm{R_d}$ for $\chi = 0$ (pure-convection heat transfer), the local Nusselt number is proportional only to the wall temperature gradient $-(1 + (4\mathrm{R_d}H^3/3))\theta'(\chi, 0)$. For the case of large H and $\mathrm{R_d}$ (radiation effects are very much pronounced), although $-(1 + (4\mathrm{R_d}H^3/3))\theta'(\chi, 0)$ is low as shown in Figs. 2b and 3b, the local Nusselt number is large. This is due to the fact that the local Nusselt number is found to be more sensitive to H and $\mathrm{R_d}$ than $-f'(\chi, 0)$, as revealed in Eqs. (12) and (13). More-

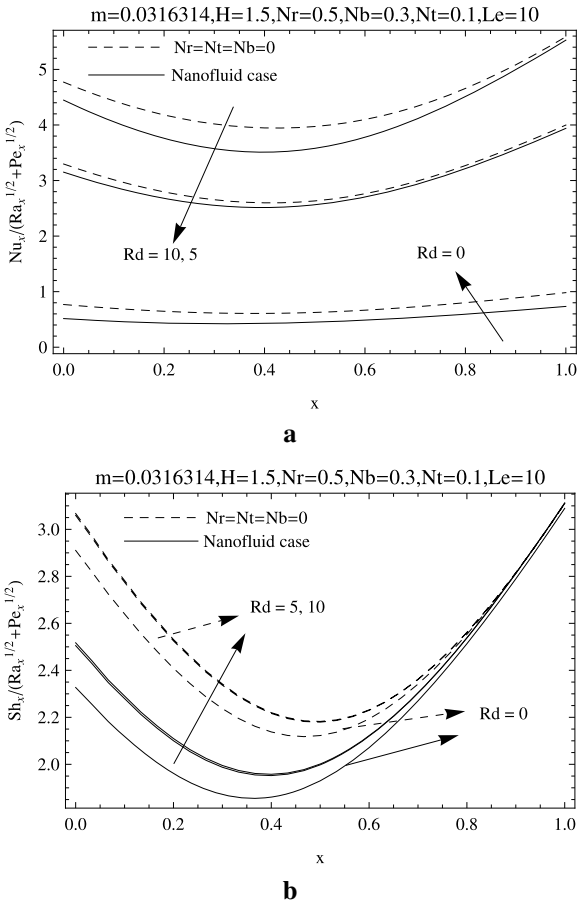

Fig. 8 Effect of R_d on **a** the local Nusselt number and **b** the local Sherwood number

over, for $\chi = 1$ (forced convection limit), the flow is uncoupled from the thermal and volume fraction buoyancy effects, and therefore, the local Sherwood number does not depend on R_d.

5 Conclusions

Numerical solutions of steady mixed convection flow of a nanofluid over a vertical cone embedded in a saturated porous medium in the presence of thermal radiation with Rosseland diffusion approximation are presented. The model used for the nanofluid incorporates the effects of Brownian motion and thermophoresis. The entire regime of mixed convection is included, as the combined convection parameter varies from 0 (pure free convection) to 1 (pure forced convection). The transformed non-linear system of equations is solved using the Keller box method. A comparison between the present (for some special cases) with previously published results are found to be in very good agreement. The numerical results are presented for the local Nusselt and the Sherwood numbers with various values of the buoyancy ratio, the Brownian motion parameter, the thermophoresis parameter the free stream velocity exponent, the radiation–conduction parameter, the surface temperature parameter, and the Lewis number. It was found that the local Nusselt number increases when any of the parameters; buoyancy ratio, the Brownian motion, the thermophoresis, the free stream velocity exponent, the radiation–conduction, the surface temperature, and the Lewis number increase. In addition, the local Sherwood number increases as the buoyancy ratio, Brownian motion parameter, Lewis number, free stream velocity exponent, radiation-conduction parameter or the surface temperature parameter increase. But quite the opposite is seen as the thermophoresis parameter increases. Furthermore, both the local Nusselt and the Sherwood numbers decrease initially, reaching to a minimum for the intermediate value of the mixed convection parameter, and then increase gradually. Moreover, it is shown that the effects of the Lewis number, and the thermophoresis parameters are more pronounced on the local Sherwood number than on the local Nusselt number. However, the effects of the radiation–conduction parameter and the surface temperature parameter are significantly stronger on the local Nusselt number than that on the local Sherwood number.

Acknowledgements The authors are thankful to the reviewers for the positive comments and the valuable suggestions, which led to definite improvement in the paper. This work is supported by the Imam Khomeini International University of Iran, under the grant 751166-91.

References

1. Nield DA, Bejan A (2006) Convection in porous media, 3rd edn. Springer, New York
2. Vafai K (2005) Handbook of porous media, 2nd edn. Taylor & Francis, New York
3. Pop I, Ingham DB (2001) Convective heat transfer: mathematical and computational modelling of viscous fluids and porous media. Pergamon, Oxford
4. Ingham DB, Pop I (1998) Transport phenomena in porous media, vol I. Pergamon, Oxford, vol II, 2002
5. Bejan A, Dincer I, Lorente S, Miguel AF, Reis AH (2004) Porous and complex flow structures in modern technologies. Springer, New York

6. Yih KA (1999) Coupled heat and mass transfer by free convection over a truncated cone in porous media: VWT/VWC or VHF/VMF. Acta Mech 137:83–97
7. Yih KA (2000) Combined heat and mass transfer in mixed convection adjacent to a VWT/VWC or VHF/VMF cone in a porous medium: the entire regime. J Porous Media 3(2):185–191
8. Cheng CY (2009) Natural convection heat and mass transfer from a vertical truncated cone in a porous medium saturated with a non-Newtonian fluid with variable wall temperature and concentration. Int Commun Heat Mass Transf 36:585–589
9. Cheng CY (2011) Soret and Dufour effects on natural convection boundary layer flow over a vertical cone in a porous medium with constant wall heat and mass fluxes. Int Commun Heat Mass Transf 38:44–48
10. Das SK, Choi SU, Yu W, Pradeep T (2008) Science and technology. Wiley-Interscience, New York
11. Buongiorno J (2006) Convective transport in nanofluids. J Heat Transf 128:241–250
12. Bianco V, Chiacchio F, Manca O, Nardini S (2009) Numerical investigation of nanofluids forced convection in circular tubes. Appl Therm Eng 29:3632–3642
13. Nield DA, Kuznetsov AV (2009) The Cheng–Minkowycz problem for natural convective boundary-layer flow in a porous medium saturated by a nanofluid. Int J Heat Mass Transf 52:5792–5795
14. Nield DA, Kuznetsov AV (2009) Thermal instability in a porous medium layer saturated by a nanofluid. Int J Heat Mass Transf 52:5796–5801
15. Kuznetsov AV, Nield DA (2010) Effect of local thermal non-equilibrium on the onset of convection in a porous medium layer saturated by a nanofluid. Transp Porous Media 83:425–436
16. Kuznetsov AV, Nield DA (2010) Thermal instability in a porous medium layer saturated by a nanofluid: Brinkman model. Transp Porous Media 81:409–422
17. Nield DA, Kuznetsov AV (2011) The effect of vertical through flow on thermal instability in a porous medium layer saturated by a nanofluid. Transp Porous Media 87:765–775
18. Xuan Y, Yu K, Li Q (2005) Investigation on flow and heat transfer of nanofluids by the thermal lattice Boltzmann model. Prog Comput Fluid Dyn 5:13–19
19. Keblinski P, Phillpot SR, Choi SUS, Eastman JA (2002) Mechanisms of heat flow in suspensions of nano-sized particles (nanofluids). Int J Heat Mass Transf 45:855–863
20. Das SK, Putra N, Thiesen P, Roetzel W (2003) Temperature dependence of thermal conductivity enhancement for nanofluids. J Heat Transf 125:567–574
21. Putra N, Roetzel W, Das SK (2003) Natural convection of nano-fluids. Heat Mass Transf 39:775–784
22. Wen D, Ding Y (2006) Natural convective heat transfer of suspensions of titanium dioxide nanoparticles (nanofluids). IEEE Trans Nanotechnol 5:220–227
23. Chamkha AJ, Aly AM, Al-Mudhaf H (2011) Laminar MHD mixed convection flow of a nanofluid along a stretching permeable surface in the presence of heat generation or absorption effects. Int J Microscale Nanoscale Thermal Fluid Transp Phenom 2: Article 3
24. Chamkha AJ, Gorla RSR, Ghodeswar K (2010) Non-similar solution for natural convective boundary layer flow over a sphere embedded in a porous medium saturated with a nanofluid. Transp Porous Media 86:13–22. doi:10.1007/s11242-010-9601-0
25. Gorla RSR, EL-Kabeir SMM, Rashad AM (2011) Heat transfer in the boundary layer on a stretching circular cylinder in a nanofluid. J Thermophys Heat Transf 25:183–186
26. Gorla RSR, Chamkha AJ, Rashad AM (2011) Mixed convective boundary layer flow over a vertical wedge embedded in a porous medium saturated with a nanofluid. J Nanoscale Res Lett 6:207
27. Chamkha AJ, Abbasbandy S, Rashad AM, Vajravelu K (2012) Radiation effects on mixed convection over a wedge embedded in a porous medium filled with a nanofluid. Transp Porous Med 91:261–279
28. Yih KA (1999) Mixed convection about a cone in a porous medium: the entire regime. Int Commun Heat Mass Transf 26:1041–1050
29. Yih KA (2001) Radiation effect on mixed convection over an isothermal wedge in porous media: the entire regime. Heat Transf Eng 22(9):26–32
30. Bakier AY (2001) Thermal radiation effect of mixed convection from vertical surfaces in saturated porous media. Int Commun Heat Mass Transf 28:119–126
31. Kumari M, Nath G (2004) Radiation effect on mixed convection from a horizontal surface in a porous medium. Mech Res Commun 31:483–491
32. Chamkha AJ, Ben-Nakhi A (2008) MHD mixed convection–radiation interaction along a permeable surface immersed in a porous medium in the presence of Soret and Dufour effects. Heat Mass Transf 44:845–856
33. Bakier AY, Rashad AM, Mansour MA (2009) Group method analysis of melting effect on MHD mixed convection flow from radiate vertical plate embedded in a saturated porous media. Commun Nonlinear Sci Numer Simul 14:2160–2170
34. Yih KA (2000) Combined heat and mass transfer in mixed convection adjacent to a VWT/VWC or VHF/VMF cone in a porous medium: the entire regime. J Porous Media 3(2):185–191
35. Yih KA (2001) Radiation effect on mixed convection over an isothermal cone in porous media. Heat Mass Transf 37:53–57
36. Hess JL, Faulkner S (1965) Accurate values of exponent governing potential flow about semi-infinite cone. AIAA J 3:767
37. Cebeci T, Bradshaw P (1984) Physical and computational aspects of convective heat transfer, 2nd edn. Springer, New York
38. Hsieh JC, Chen TS, Armaly BF (1993) Mixed convection along a nonisothermal vertical flat plate embedded in a porous medium: the entire regime. Int J Heat Mass Transf 36:1819–1825
39. Kumari M, Gorla RSR (1997) Combined convection along a non-isothermal wedge in a porous medium. Heat Mass Transf 32:393–398